Synthetic and Systems Biotechnology 8 (2023) 148–156

Contents lists available at ScienceDirect

Synthetic and Systems Biotechnology

journal homepage: www.keaipublishing.com/en/journals/synthetic-and-systems-biotechnology

Single and multiplexed gene repression in solventogenic *Clostridium* via Cas12a-based CRISPR interference

Rochelle Carla Joseph , Nicholas R. Sandoval *

Department of Chemical and Biomolecular Engineering, Tulane University, New Orleans, LA, 70118, United States

ARTICLE INFO

Keywords:
CRISPR Cas12a
Clostridium
CRISPRi

ABSTRACT

The Gram-positive, spore-forming, obligate anaerobic firmicute species that make up the *Clostridium* genus have broad feedstock consumption capabilities and produce value-added metabolic products, but genetic manipulation is difficult, limiting their broad appeal. CRISPR-Cas systems have recently been applied to *Clostridium* species, primarily using Cas9 as a counterselection marker in conjunction with plasmid-based homologous recombination. CRISPR interference is a method that reduces gene expression of specific genes via precision targeting of a nuclease deficient Cas effector protein. Here, we develop a dCas12a-based CRISPR interference system for transcriptional gene repression in multiple mesophilic *Clostridium* species. We show the *Francisella novicida* Cas12a-based system has a broader applicability due to the low GC content in *Clostridium* species compared to CRISPR Cas systems derived from other bacteria. We demonstrate >99% reduction in transcript levels of targeted genes in *Clostridium acetobutylicum* and >75% reduction in *Clostridium pasteurianum*. We also demonstrate multiplexed repression via use of a single synthetic CRISPR array, achieving 99% reduction in targeted gene expression and elucidating a unique metabolic profile for their reduced expression. Overall, this work builds a foundation for high throughput genetic screens without genetic editing, a key limitation in current screening methods used in the *Clostridium* community.

1. Introduction

The *Clostridium* genus consists of a group of Gram-positive, obligate anaerobic firmicutes. Among this group are multiple industrially relevant strains known for their potential as therapeutics and their ability to degrade cellulosic biomass, fix carbon, and to produce biofuels and other platform chemicals [1,2]. With low unmodified *Clostridium* strain product yields and titers [3], strain improvement represents an attractive path toward production of value added biofuels and chemicals. While genetic manipulations have produced desirable phenotypes in *Clostridium* species including improved butanol production [4–6], the established methods of genetic editing are time-consuming, labor-intensive and require translatable knowledge of biochemical pathways and regulatory mechanisms. Multiple genes, as well as the function of their respective proteins, remain uncharacterized across *Clostridium* species [7–9]. A better understanding of *Clostridium* physiology is necessary for better combatting *Clostridial* infections, the development of higher-producing strains, and the general utility of *Clostridium* in industry. Improvements, such as a more detailed characterization of pathogenesis, regulation of sugar metabolism, and of the sporulation cascade and its downstream regulon [10] would prove useful toward these goals.

The development of tools for rapid and systemic manipulation of gene expression in *Clostridium* are valuable for the isolation of desirable phenotypes and understanding genotype-phenotype relationships [11,12]. Long-established methods to study gene function rely heavily on plasmid-based homologous recombination for gene knockouts and stable gene overexpression [13,14], and transposon-based gene disruption methods [15], allowing single-edit events only after multiple rounds of cloning. Gene knockdowns can be implemented using antisense RNAs (asRNAs), but asRNAs have been shown to be promiscuous even though large constructs (>100 bases) are required for gene repression [16–18].

CRISPR-based systems have been established as powerful tools for genetic manipulation in various organisms including non-model bacteria such as *Clostridium* [11]. Among them, the commonly used CRISPR Class 2 type II *Spy*Cas9 protein recognizes a simple protospacer adjacent motif (PAM) sequence (5′-NGG-3′), and when bound to a guide RNA is the sole protein required for targeted endonuclease activity [19]. Unlike *Spy*Cas9, the Class 2 Type V Cas12a CRISPR effector proteins recognize

Peer review under responsibility of KeAi Communications Co., Ltd.

* Corresponding author. Department of Chemical and Biomolecular Engineering, Tulane University, St. Charles Ave, New Orleans, LA, 70118, United States.
E-mail address: nsandova@tulane.edu (N.R. Sandoval).

https://doi.org/10.1016/j.synbio.2022.12.005
Received 12 August 2022; Received in revised form 28 November 2022; Accepted 20 December 2022
Available online 24 December 2022

Abbreviations

Cac	*Clostridium acetobutylicum*
Cpa	*Clostridium pasteurianum*
CGM	Clostridium Growth Medium
CRISPR	clustered regularly interspaced short palindromic repeats
PAM	protospacer adjacent motif
RBS	ribosomal binding site

T-rich PAM sites and can process multiple crRNAs from a single precursor CRISPR RNA (pre crRNA) transcript [20,21]. *Fn*Cas12a, derived from *Francisella novicida,* recognizes the PAM site 5′-TTN-3′, the shortest and simplest of known Cas12a proteins, although several studies have demonstrated system-specific improvement of *Fn*Cas12a efficiency with more stringent PAM sites such as 'YTV' [22,23], 'KYTV' [24], and 'TTTV' [25–27]. *Clostridium* genomes are highly AT-rich, having only approximately 30% GC content and CRISPR-Cas12a systems derived from various bacteria have been used to facilitate gene deletion in several *Clostridium* species including *Clostridium beijerinckii* and *C. ljungdahlii* [28].

Catalytically dead Cas effectors, such as dCas9 and dCas12a have no endonuclease activity and repress gene expression by binding to a target region defined by a gRNA, thereby sterically hindering the activity of RNA polymerase [29]. dCas12a, and other effector proteins capable of processing their own CRISPR array, additionally allow the concurrent targeted repression of multiple genes through the expression of a single synthetic array. The use of catalytically dead Cas effectors for gene repression allows rapid elucidation of genotype-to-phenotype relationships while circumventing the challenges associated with gene knockouts, which are labor intensive and are limited to the study of non-essential genes. Both dCas9 and dCas12a have been used for gene repression in *Clostridium* species. However, the use of dCas12a has been limited to *C. ljungdahlii* and its ability to easily and simultaneously target multiple genes remains untapped [30].

Here, we expand the use of dCas12a for transcriptional gene repression in two additional species: *Clostridium acetobutylicum (Cac)* and *C. pasteurianum (Cpa)*. We show that based on PAM site availability, d*Fn*Cas12a is the most suited CRISPR effector for modulating gene expression in *Clostridium* species. We utilize the d*Fn*Cas12a protein to demonstrate single- and multiplexed repression through the analysis of mRNA expression and further demonstrate the ability of our CRISPR-d*Fn*Cas12a system to redirect metabolic flux through the analysis of metabolites. CRISPR-based tools are a valuable addition to the *Clostridium* genetic engineering toolkits. The use of d*Fn*Cas12a for gene repression improves the genome coverage available for genetic manipulation and creates a foundation for high throughput genetic screens, which would prove to be a significant improvement over current screening methods currently used in the *Clostridium* community.

2. Materials and methods

2.1. Analysis of PAM sites in Clostridium genomes

Protospacer Adjacent Motif (PAM) site analysis was performed using a custom python script designed to interrogate imported genomes to determine the number of and distance between sequential occurrences of the consensus PAM sequence for respective CRISPR associated effector proteins. Briefly, FASTA genome sequences obtained from NCBI were sequentially scanned for PAM sequences and their reverse complements (for valid PAM sites on the opposite strand). Once a PAM site was identified, the number of bases from the end of one to the beginning of the next is reported as the distance between PAM sites. Overlapping PAM sites return a value of 0 bp distance. Data was outputted as the number of PAM sites as a function of distance between PAM sites. The availability of nine PAM sequences, recognized by various Cas9 and Cas12a proteins was screened: TTN (*Francisella novicida*), TTTV (*Acidaminococcus* sp., *Lachnospiraceae bacterium*) [20], TYCV (*As*Cas12a, *Lb*Cas12a RR variant) [31], TATV (*As*Cas12a RVR variant) [31], NGG (*Streptococcus pyogenes*) [19], NNGRRN (*Staphylococcus aureus*) [32], NNNNGATT (*Neisseria meningitidis*) [33], NNAGAAW (*Streptococcus thermophilus*) [34], NAAAAC (*Treponema denticola*) [35].

2.2. Strains, media, and reagents

Strains, plasmids and oligonucleotides used in this study are listed in the supplementary material in Tables S1–S4 respectively. *Clostridium pasteurianum* ATCC 6013 (*Cpa*) and *Clostridium acetobutylicum* ATCC 824 (*Cac*) were grown at 37 °C under anaerobic conditions (Coy Labs type B vinyl anaerobic chamber with artificial atmosphere containing 7% H_2, 5% CO_2, 88% N_2 and O_2 levels not exceeding 25 ppm during culturing) in 2xYTG medium (per liter: tryptone, 16 g; yeast extract, 10 g; sodium chloride, 4 g; glucose, 5 g; titrated to pH 6.5), Clostridium Growth Medium (per liter: KH_2PO_4, 0.75 g; K_2HPO_4, 0.75 g; $MgSO_4$ [anhydrous], 0.348 g; $MnSO_4{\cdot}H_2O$, 0.01 g; $FeSO_4{\cdot}7H_2O$, 0.01 g; NaCl, 1.0 g; asparagine, 2.0 g; yeast extract, 5.0 g; sodium acetate, 2.46 g; $(NH_4)_2SO_4$, 2.0 g; and *para*-aminobenzoic acid [PABA], 0.04 g; titrated to pH 6.8) and on solid 2xYTG agar plates supplemented with thiamphenicol (15 μg/mL) where appropriate. *Cac* and *Cpa* strains were stored at −80 °C in 2xYTG supplemented with 15% glycerol and were revived by plating onto 2xYTG agar plates. Gene repression assays were performed in fresh CGM, 2xYTG or P2Y (per liter: ammonium chloride, 1.6 g; sodium Acetate, 2.46 g; potassium phosphate monobasic, 0.5 g; potassium phosphate dibasic, 0.5 g; magnesium sulfate heptahydrate, 2 g; manganese sulfate monohydrate, 0.1 g; sodium chloride, 0.1 g; iron sulfate heptahydrate 0.1 g; *p*-aminobenzoic acid, 0.1 g; thiamine, 0.1 g; biotin, 0.01 g; 1 g/L yeast extract; 60 g/L glycerol or 30 g/L glucose as appropriate).

Escherichia coli 10β strains were grown aerobically at 37 °C in liquid Lysogeny Broth (LB) or on solid LB agar plates supplemented with the appropriate antibiotic (35 μg/mL chloramphenicol, 25 μg/mL kanamycin). *E. coli* strains were stored at −80 °C in LB medium supplemented with glycerol to a final concentration of 20%.

Plasmid extractions and DNA purifications were performed using Qiaprep Spin Miniprep and QIAquick PCR Purification kits respectively (Qiagen). Enzymes used in the construction of plasmids including DNA amplification (Q5 High-Fidelity DNA polymerase), restriction digest enzymes and Instant Sicky End Ligase was obtained from New England Biolabs. Oligonucleotides were synthesized by Integrated DNA Technologies.

2.3. Construction of plasmids

The *bgaL* promoter and the *bgaR* gene encoding the regulator, d*Fn*Cas12a gene and *Fn*Cas12a scaffold were cloned into the pMTL85141 [36] shuttle vector to produce pJRJ001. d*Fn*Cas12a was codon optimized for expression in *Clostridium* (IDT codon optimization tool) and chemically synthesized as gene fragments (Twist Bioscience). The *bgaL* promoter and *bgaR* gene were amplified from the pKOD_mazF plasmid [13] using primers 138 and 139 and the *Fn*Cas12a scaffold, directly followed by a *lacZα* gene, was synthesized as fragments (gBlocks, IDT) and PCR amplified using primers 144 and 171. Fragments were inserted into pMTL85141 via restriction cloning (*Not*I, *Sal*I, *Asc*I). Target sequences (Table S4) were inserted to pJRJ001 via golden gate cloning [37]. Briefly, target sequences were inserted immediately downstream of *Fn*Cas12a scaffold sequence by annealing a complementary pair of ssDNA oligos with appropriate overhangs and ligating with the d*Fn*Cas12a vector digested with *Bsa*I.

2.4. Plasmid transfer into Clostridium spp.

Electrocompetent *C. acetobutylicum* cells were prepared and transformed as described by Mermelstein *et al.* [38] with few changes. In short, an overnight culture of OD_{600} 0.4–0.8 was diluted in 100 mL fresh 2xYTG media to a starting OD_{600} of 0.05. The culture was grown at 37 °C and harvested at late exponential phase (OD_{600} = 0.6–0.8) by first centrifuging the cells for 10 min at 6000×*g* and 4 °C, washing the pellet with electroporation buffer (272 mM sucrose, 5 mM NaH_2PO_4) then resuspending in 4 mL of the same buffer.

Before transformation into *C. acetobutylicum*, plasmids were transformed into electrocompetent *E. coli* harboring the pAN3 vector encoding the *Bacillus subtilis* phage Φ3T I methyltransferase for *in vivo* methylation [13,39]. Plasmids were isolated using QIAprep spin miniprep kit (Qiagen). Electrocompetent *C. acetobutylicum* cells were transformed by adding 0.5–2 μg of methylated DNA to 0.7 mL of electrocompetent cells in a 4 mm cuvette and electroporating with settings 2 kV, infinite resistance and 25 μF capacitance. The electroporated cells were immediately recovered in 10 mL of 2xYTG pre-warmed to 37 °C and incubated for 4 h at 37 before plating on warm RCM solid media supplemented with thiamphenicol.

Electrocompetent *C. pasteurianum* cells were prepared and transformed according to Pyne *et al.* [40]. As with *Cac*, an overnight *Cpa* culture was diluted in fresh 2xYTG to a starting OD_{600} of 0.05 and grown to an OD600 between 0.3 and 0.4 at which point sucrose and glycine were added to a final concentration 0.4 M and 0.2 M respectively. The culture was harvested at late exponential phase (OD_{600} = 0.6–0.8) by first centrifuging for 10 min at 4000×*g* and 4 °C, washing the pellet with SMP buffer (270 mM sucrose, 1 mM $MgCl_2$, 5 mM NaH_2PO_4) then resuspending the cells in 3 mL of the same buffer.

For *in vivo* plasmid methylation, plasmids were transformed into *E. coli* cells harboring pCpaDcm2.0 [41]. Overnight cultures were supplemented with 1 mM rhamnose and methylated plasmids were isolated using QIAprep spin miniprep kit. Cells were transformed by adding 20 μL of methylated DNA to a total 0.5–2 μg and 30 μL of 100% ethanol to 680 μL of electrocompetent cells in a 4 mm cuvette and electroporating with settings 1.8 kV, infinite resistance and 25 μF capacitance. The electroporated cells were immediately recovered in 10 mL of pre-warmed recovery media (2xYPG with 0.2 M Sucrose) and incubated for 16 h at 37 °C before plating on warm RCM solid media supplemented with thiamphenicol.

2.5. Gene repression assays

Gene repression assays were performed by inoculating overnight cultures (OD = 0.4–0.8) into fresh media supplemented with lactose to a final concentration of 10 mM to induce d*Fn*Cas12a expression. Samples for turbidity, metabolite analysis, and mRNA analysis were taken simultaneously. Cell density was measured by absorbance at 600 nm using a spectrophotometer (Biowave CO8000). Metabolites were analyzed via liquid chromatography. Refractive index analysis of supernatant from culture samples was performed for acetate, butyrate, butanol, ethanol, lactose, 1,3-propanediol, glucose and glycerol on a Waters Acquity UPLC chromatography system (with Waters Empower 3 Software) using an ion exclusion column (80 °C with 0.4 mL/min 5 mM sulfuric acid mobile phase). All samples passed through a 0.22 μm filter (VWR) after centrifugation for 1 min at 17,000×*g* to remove live cells.

2.6. RNA isolation and analysis of mRNA expression

mRNA levels were analyzed via RT-qPCR using iTaq Universal SYBR Green Supermix (Bio-Rad) in 10 μL reactions using 2 μL of cDNA as template following the manufacturer's directions and using the MIQE guidelines [42] as a guide. Reactions were run on a CFX96 Touch Real-Time PCR Detection System (Bio-Rad). Samples were run in technical duplicate to account for data variability. To ensure that changes observed were due to CRISPRi activity we ran suitable controls including a minus reverse transcription control, minus template control and minus amplification (no iTaq) control. Primers for RT-qPCR are listed in Table S2. Amplicons were between 90 and 150 bases and located within the coding region of the gene. The *fabZ* and *recA* genes were used as references for *Cac* and *fabz* was used for *Cpa* RNA analysis based on previous studies.

RNA was isolated as described by Jones *et al.* [43]. Briefly, samples were collected and cell pellets were stored at −80 °C for up to one month. Cells were washed in 1 ml SET buffer (25% sucrose, 50 mM EDTA [pH 8.0], and 50 mM Tris-HCl [pH 8.0]) prior to RNA isolation then resuspended in 220 μL SET buffer with 20 mg/mL lysozyme and 4.55 U/mL proteinase K (VWR) and incubated at room temperature for 6 min. Following incubation, 40–50 mg of acid-washed glass beads (≤106 μm; Sigma) were added to the solution, and the mixture was continuously vortexed for 4 min at room temperature. 1 mL of ice cold TRIzol (Invitrogen) was added and 500 μL of sample was diluted with an equal volume of ice cold TRIzol. Following dilution, 200 μL of ice-cold chloroform was added to each sample, mixed vigorously for 15 s, and incubated at room temperature for 3 min. Samples were then centrifuged at 17,000×*g* for 15 min at 4 °C. The upper phase was saved and diluted by adding 500 μL of 70% ethanol. Samples were immediately applied to the RNeasy Mini Kit (Qiagen). To minimize genomic DNA contamination, samples were incubated with the wash buffer at room temperature for 4 min and treated with DNase (Qiagen) as per manufacturer's instructions.

The RNA was resuspended in RNase-free water and quantitated in a spectrophotometer (DeNovix DS-11). Only samples with a 260/280 ration above 1.8 was used for analysis. cDNA was synthesized, in technical duplicates, using an iScript cDNA synthesis kit (Bio-Rad) and 500 ng of RNA as a template.

2.7. Statistical analysis

Statistical tests were performed using Excel and Graphpad Prism. Results were deemed statistically significant for comparisons with P-value <0.05. Statistical significance is indicated in each figure where applicable. Figures were created using Graphpad prism and Biorender.com.

3. Results

3.1. FnCas12a allows maximum targeting coverage in Clostridium spp. based on PAM site availability

To determine the most suitable CRISPR associated effector protein for use in *Clostridium* based on genome targeting coverage, we surveyed the genomes of several species including *C. acetobutylicum*, *C. pastuerianum*, *C. biejerinckii,* and *C. ljungdahlii* for PAM sequences of Cas9 and Cas12a proteins from various species. Among all PAM sites tested, TTN, recognized by *Fn*Cas12a, was most abundant in all genomes tested and was present with the least distance between successive PAM sites, on average 1 PAM occurrence every 2 base pairs. Additionally, compared to the NGG consensus recognized by the more commonly used *Spy*Cas9, available TTN PAM sites within *Clostridium* genomes are typically located within 40 bases (99% of TTN PAM sites in *Cac*) of each other allowing uniform targeting coverage of the genome (Fig. 1, S1). On the other hand, unavailability of PAM sites within a 40-base pair range on the *Cac* genome increases to 16% and 33% respectively when TTTV and NGG PAM sequences are considered.

The TTTV PAM motif, a more stringent site recognized by Cas12a proteins in general [20], has been reported to result in higher activity in *Fn*Cas12a than TTN [44]. To balance the need for precise d*Fn*Cas12a targeting and PAM site availability, we opted to use the functional TTV PAM site and when possible TTTV (Table S4).

While the increased PAM site availability potentially increases the

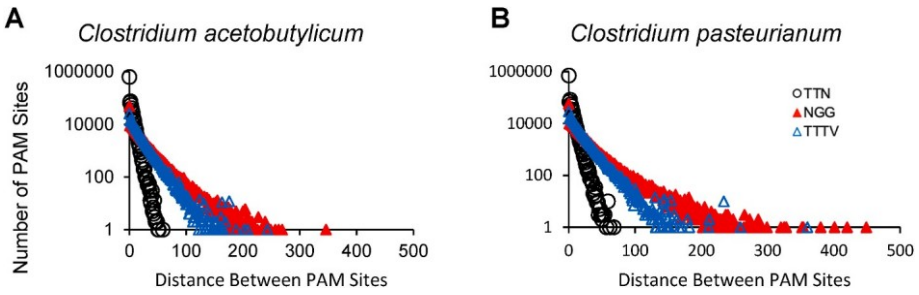

Fig. 1. Distribution of TTN, TTTV and NGG PAM sites in (A) *Clostridium acetobutylicym* and (B) *Clostridium pasteurianum*: Graph shows distribution of PAM consensus sequences within 500 bp of each other. PAM site data was obtained using a python script designed to scan genomes and determine the number of and distance between sequential occurrences of the consensus sequence for respective Cas proteins.

chance of off-target effects with use of *Fn*Cas12a in *Clostridium*, the effects of mismatches, additions, and deletions of bases in the target region of the crRNA with regards to Cas12a activity has been widely studied [44–46] and off-target effects can be minimized by carefully selecting target sequences. Additionally, off-target effects have a reduced impact in CRISPRi applications, as these interactions do not result in permanent alterations to the genome, as a dsDNA break would.

3.2. dFnCas12a enables regulation of endogenous genes in Clostridium acetobutylicum

We aimed to control the expression of genes in *Clostridium* species using d*Fn*Cas12a. To determine whether d*Fn*Cas12a could be used to repress gene expression in *Cac,* we first constructed plasmids containing the d*Fn*Cas12a gene and the *Fn*Cas12a scaffold along with a 20-base target sequence. d*Fn*Cas12a was placed under the control of a lactose-inducible promoter (*bgaL* in conjunction with the gene encoding the corresponding transcriptional regulator, *bgaR*) to avoid possible toxicity [47–49], and to minimize metabolic burden on the cells. However, we found that early induction of d*Fn*Cas12a had no significant effect on growth (Fig. S2), with successful repression resulting in decreased transcription of target genes and, in general, observation of expected phenotype.

As a proof of concept, we chose to target the *spo0A* gene. Spo0A is a master regulator, playing a crucial role in initiating sporulation, as well as controlling the shift from acidogenesis to solventogenesis in *Cac*. Both overexpression and deletion of *spo0A* in *Cac* have been previously characterized, having resulted in increased and reduced solvent production respectively [50]. We therefore expected that CRISPR-based downregulation of *spo0A* would also result in the reduction of solvent production, an easily detectable phenotype.

To begin, we designed four crRNA sequences within 100 nucleotides of the translational start site to target the *spo0A* gene. *Spo0A* expression is highly regulated and consensus sequences for identified *sigA*, *sigK* and *sigH* binding sites, as well as an 0A box have been identified upstream of the *spo0A* open reading frame [51]. CRISPRi activity has been shown to be particularly dependent on target region [30,52], and the effect of regulatory elements on binding activity of the Cas effector has not been extensively studied [53]. Therefore, two crRNAs, g39 and g64 targeted the region between the *sigA*/*sigK* and *sigH* consensus sequences, g40 targeted the *sigH* region and g41 targeted the *spo0A* open reading frame (Fig. S3A, Table S4). Because the role of Spo0A in *Cac* metabolite production is well characterized, we first evaluated metabolic profile as a measure of successful gene repression then selected one of the cultures with the expected phenotype to assess transcriptional levels of *spo0A*, confirming that the observed phenotypical change was associated with the repression of the target gene.

In our preliminary studies, we observed the expected phenotype for *spo0A* downregulation using targets 39 and 64, while the use of the g41 resulted in no significant difference in metabolic profile when compared to a no plasmid control. Targeting d*Fn*Cas12a with g40 unexpectedly resulted in increased butanol and acetone levels compared to a no plasmid control (although not statistically significant). Additionally, a synthetic CRISPR array simultaneously expressing g39 and g64 (g65) resulted in metabolic profiles that were similar to that of the cultures where only a single crRNA was employed. Unexpectedly, expressing both g39 and g40 (g66) resulted in a metabolic profile similar to the no target control (Fig. S3B). We also observed a small but significant increase in ethanol with all crRNAs expressed compared to the no plasmid control (Fig. S3). Although unexpected, this difference in ethanol production was not observed in the time course experiment with a non-targeting crRNA as a control (Fig. 2G). Thus, this difference may be due to an unintended effect of plasmid burden.

To confirm d*Fn*Cas12a activity, we cultured *Cac* cells harboring the pJRJ001-g39 over a 96-h period in order to determine both metabolic and transcriptional profiles following d*Fn*Cas12a induction. As a control, we replaced the target region with a random non-targeting 20-base sequence subsequently referred to as the No Target control in this study. Using g39 to target the *spo0A* gene, we saw a reduction in butanol and acetone production to undetectable levels, while a 2.2-fold increase in butyrate production was observed (Fig. 2D) after 96-h growth compared to the No Target control, whose metabolic profile varied between biological replicates, likely due to uncontrolled fermentation conditions. Analysis of mRNA extracted from samples 24 h after d*Fn*Cas12a induction shows 92% reduction in *spo0A* transcription. Consistent with previous studies, we also observed a marked decrease (>99%) of *adc* and the genes of the *sol* operon (*ctfa*, *ctfb*, *adhE2*), which encode the proteins necessary for butanol and acetone production (Fig. 2A).

3.3. dFnCas12a modulates the expression of multiple genes using a single CRISPR array

Next, we aimed to investigate the ability for d*Fn*Cas12a-based multiplexed gene repression through the expression of a single CRISPR array. To test this, we simultaneously targeted a pair of decarboxylases, *adc* and *pdc* in *Clostridium acetobutylicum*. For each gene, we selected a single target downstream of the transcriptional start site but upstream of the open reading frame targeting the antisense strand (Fig. S4A).

Acetoacetate decarboxylase (Adc) catalyzes the second step of acetone production from acetoacetyl-CoA. Accordingly, previous *adc* knockouts have resulted in the reduction of acetone production [54]. Targeting *adc*, using g74 (Table S4), we achieved 75% reduction in acetone production compared to the no target control. Consistent with previous studies, we also observed a 1.75-fold increase in acid production, 3-fold decrease in alcohol production, and reduced consumption of glucose (Fig. 3, S4C).

Pyruvate decarboxylase (Pdc) is a well characterized protein in several species and catalyzes the decarboxylation of pyruvate to acetaldehyde along the ethanol production pathway [55–58]. While a *pdc* knockout strain has not been characterized in *Clostridium*, previous studies in *C. acetobutylicum* have demonstrated high expression of *pdc* during the switch from acidogenesis to solventogenesis [59].

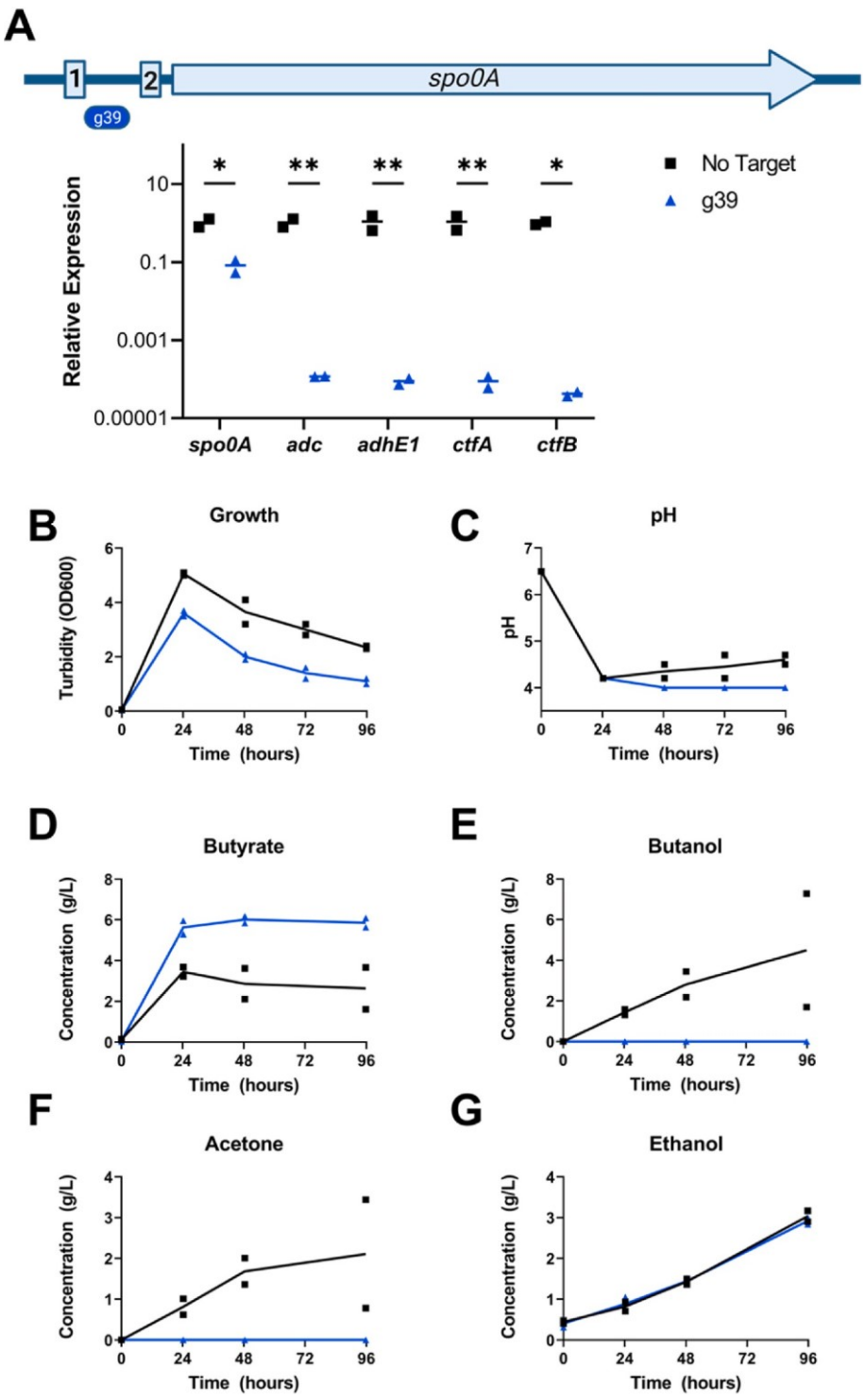

Fig. 2. Repression of *spo0A* using d*Fn*Cas12a in *Clostridium acetobutylicum*: **(A)** Transcriptional changes in *spo0A*, *adc*, *adhE1*, *ctfA* and *ctfB* following CRISPR-based repression of *spo0A*. Samples were obtained 24 h after induction of d*Fn*Cas12a with 10 mM lactose for RT-qPCR analysis. d*Fn*Cas12a targets the antisense strand, upstream of transcriptional start site between the sigma A/sigma K binding sites **(1)** and sigma H binding site/0A box **(2)** using g39 as shown. Lines are indicative of mean relative expression. **(B)** Growth, **(C)** pH and **(D–G)** metabolite production data over a 96-h fermentation following d*Fn*Cas12a induction at t = 0. All data are representative of biological duplicates. pJRJ001-g58, harboring a non-complementary gRNA sequence, is used as the no target control. *p value summary: *p < 0.05, **p < 0.01.*

Additionally, the expression of heterologous *pdc* genes in *C. acetobutylicum* and *C. thermocellum* has resulted in increased ethanol production in both species, as well as increased acetone and butanol production in *C. acetobutylicum* [60,61]. In this study, no significant difference in metabolite production, was observed when *pdc* is targeted on its own via g73 (Fig. 3, Table S4).

For multiplexed repression, we first constructed a single CRISPR array (g76) containing target sequences for both *pdc* and *adc* respectively via a single golden-gate assembly reaction. We observed over 99% reduction of both *pdc* and *adc* gene expression compared to a no target control in samples taken 24 h after d*Fn*Cas12a expression was induced (Fig. 3A). In contrast to the individual *pdc* and *adc* targets, simultaneous reduction of *pdc* and *adc* resulted in a unique phenotype, with cells showing no detectable acetone or butanol production after a 72-h fermentation (Fig. 3B).

3.4. dFnCas12a enables regulation of endogenous genes in Clostridium pasteurianum

Further, to demonstrate broad use of this system among mesophilic

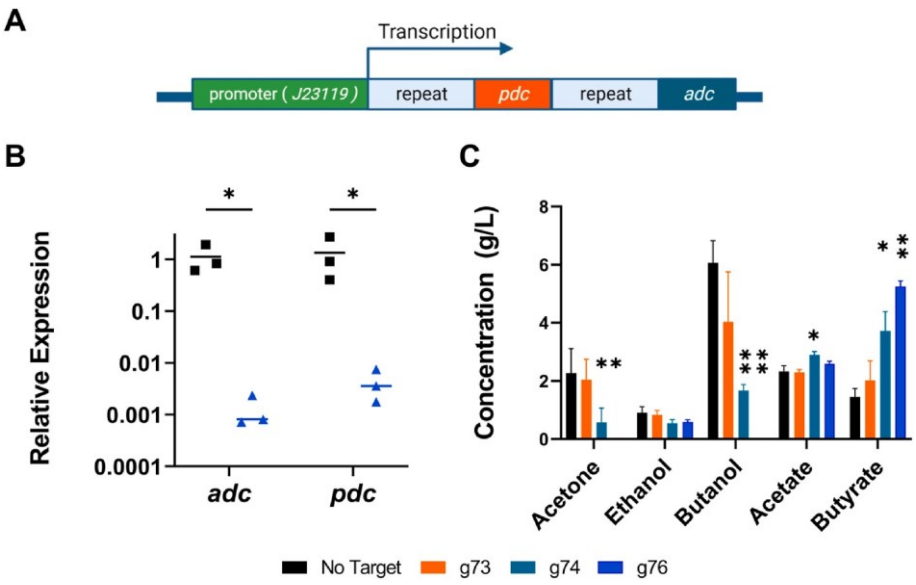

Fig. 3. Simultaneous repression of *pdc* and *adc* expression in *Clostridium acetobutylicum* using a single CRISPR array: **(A)** Map of synthetic CRISPR array **(B)** Transcriptional changes in *adc* and *pdc* following simultaneous repression of the two genes via a synthetic CRISPR array (g76). Samples were obtained 24 h after induction of d*Fn*Cas12a with 10 mM lactose for RT-qPCR analysis. Lines indicate the mean relative expression. **(C)** Concentration of acids and solvents produced when *pdc* (g73) and *adc* (g74) are targeted for repression individually, and simultaneously via a synthetic CRISPR array. Samples were obtained 72 h following d*Fn*Cas12a induction at t = 0. All data are representative of biological triplicates. Error bars indicate standard deviation. pJRJ001-g58 is used as the no target control. *p value summary: *p < 0.05, **p < 0.01*.

Clostridium species, we aimed to modulate gene expression in *Clostridium pasteurianum* using our d*Fn*Cas12a-based repression system. We first targeted *hydA* for gene repression since *hydA* has been both deleted [62] and its expression downregulated via asRNA technology [18] in previous studies. To test our system, we selected a single target, g58, directly upstream of the open reading frame on the antisense strand (Fig. 4, Table S4).

The hydrogenase A protein is responsible for maintaining redox balance in cells through the production of hydrogen gas and regeneration of NAD+. Using our d*Fn*Cas12a-based system, we were able to achieve 77% reduction of the *hydA* mRNA transcript. However, no significant change in metabolic profile was observed when *hydA* was downregulated compared to a no target control (Fig. 4).

We also targeted the *dhaB* and *dhaT2* genes of the *dha* operon. *dhaB* is the first gene in the operon and one of the genes encoding the DhaBCE protein which catalyzes the production of 3-hydroxypropanal from glycerol, and *dhaT* encodes the 1,3-propanediol dehydrogenase protein which catalyzes the final step of PDO production. Because the *dha* operon is tightly regulated, and its regulatory elements have not been well annotated, we designed four crRNAs (g26, g27, g28, g29) targeting directly upstream the open reading frames of our target genes on each strand (Fig. 5A, Table S4).

Because 1,3-PDO production is crucial to redox balance during glycerol fermentation in *Cpa*, we first induced d*Fn*Cas12a expression 4 h after inoculating overnight cultures into fresh media. We observed statistically significant reduction in 1,3-propanediol production within 4 h of d*Fn*Cas12a induction only when the antisense strand was targeted (Fig. 5B). However, 1,3-PDO production varied widely among sample replicates. On average, we observed highest reduction in 1,3-PDO production in cultures where the cells harbored pJRJ001-g26 as and cultured these colonies for further characterization.

To determine whether our system could be used to completely abolish 1,3-PDO production, we cultured cells harboring the pJRJ001-g26 plasmid over a 72-h period, inducing dFnCas12a expression immediately upon inoculating overnight cultures into fresh media. Surprisingly, we observed no significant difference in metabolite

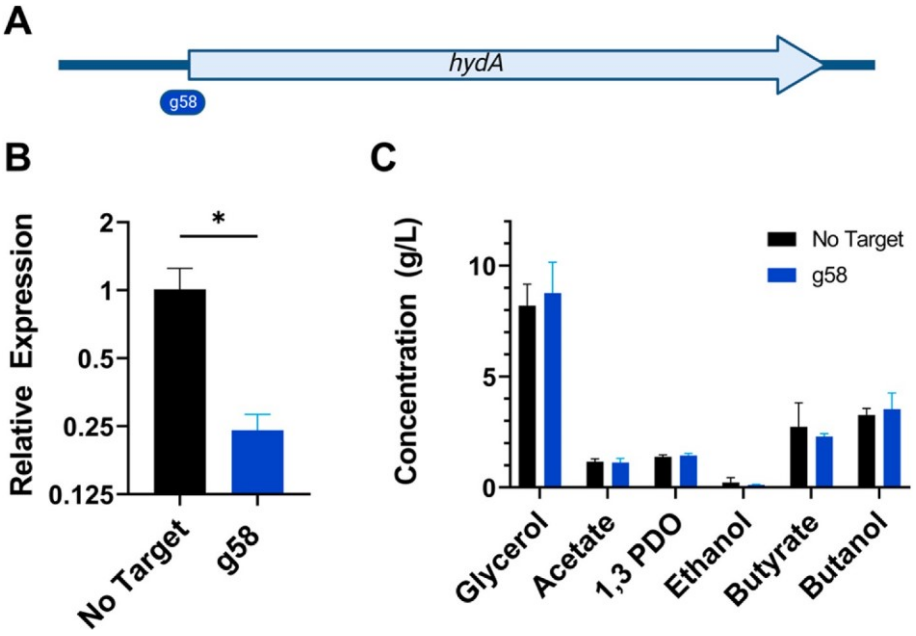

Fig. 4. Repression of *hydA* using d*Fn*Cas12a in *Clostridium pasteurianum*: **(A)** Map showing gRNA target region **(B)** Transcriptional changes in *hydA* (g58) following CRISPR-based repression. Samples were obtained 48-h after induction of d*Fn*Cas12a with 10 mM lactose for RT-qPCR analysis. Data are representative of biological duplicates. Error bars indicate standard deviation. pJRJ001-g1, harboring a non-complementary gRNA sequence, is used as the no target control *p value summary: *p < 0.05, **p < 0.01*. **(C)** Glycerol consumption and metabolite production 72 h after d*Fn*Cas12a induction. Data are representative of triplicates. No significant change in metabolite profile was observed.

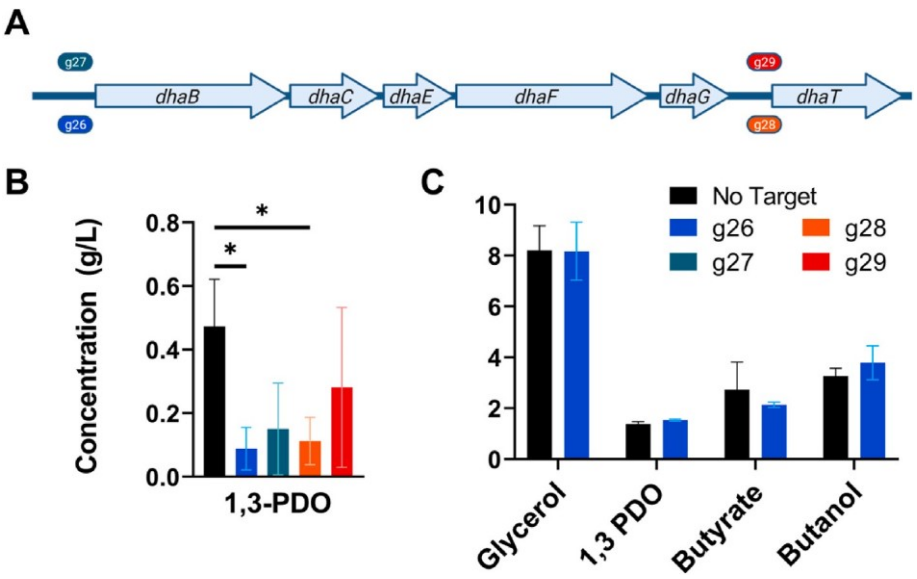

Fig. 5. Gene repression of *dha* operon in *Clostridium pasteurianum* following CRISPR-based repression of *dhaB* and *dhaT*: (A) gRNAs were designed to target sense and antisense strands of *dhaB* and *dhaT* gene respectively (B) 1,3-Propanediol concentrations following d*Fn*Cas12a expression. Samples were obtained 4 h after induction of d*Fn*Cas12a expression with 10 mM lactose. Lactose was added to media at mid-exponential phase (t = 4 h). control *p value summary: *p < 0.05, **p < 0.01*. (C) Concentrations of glycerol and metabolites produced over a 72-h fermentation of cells harboring pJRJ001-g26 following induction of d*Fn*Cas12a at t = 0 with 10 mM lactose. No significant change in metabolite profile was observed. All data are representative of triplicates. Error bars indicate standard deviation. pJRJ001-g52 is used as the no target control.

production, compared to our control when these cells were grown in CGM, 2xYTG or P2Y media over the fermentation period (Fig. 5C, S5). Additionally, transcriptional analysis of samples taken 24 h after d*Fn*Cas12a induction showed that while d*Fn*Cas12a RNA levels remained almost consistent in both the no target control and experimental samples, no significant difference in *dhaB* RNA levels was observed when *dhaB* was targeted for repression using g26.

4. Discussion

4.1. dFnCas12a enables transcriptional regulation of gene expression in Clostridium spp.

We were able to successfully repress gene expression using d*Fn*Cas12a in both *Clostridium pasteurianum* and *Clostridium acetobutylicum*. As proof of concept, we chose to target genes whose knock-out phenotypes had already been well characterized as to have a clear measure of success for our d*Fn*Cas12a-based system. In most cases, we induced d*Fn*Cas12a expression upon inoculation into fresh media to minimize expression of target genes and to achieve as close as possible to the knockout phenotype. Early induction of d*Fn*Cas12a would be necessary for maximum reduction of gene expression when targeting *spo0A*, for example, which is expressed, under the control of various promoters, throughout the life cycle of *Clostridium acetobutylicum* [51] (Fig. S3). In *Cac*, the metabolic profiles we observed were consistent with earlier studies, and alongside mRNA levels, demonstrate successful modulation of gene expression using d*Fn*Cas12a, and that in many cases, successful genotype-to-phenotype characterizations can be made using this system rather than constructing knockout strains.

Previous studies in *Cac* using d*Spy*Cas9 have shown varied degrees of repression (45–90%) via different methods of detection [11]. Particularly, the use of a d*Spy*Cas9-based CRISPRi system was employed for the repression of *spo0A* resulting in 45% reduction of mRNA levels and 58% reduction of solvent production in samples obtained after 24 h of fermentation [63], while we saw up to 90% transcript reduction and no detectable levels of acetone or butanol. However, the difference in *spo0A* repression between the two CRISPR systems may simply be a result of factors such as target position and growth medium. Another study using d*Spy*Cas9 targeting an anaerobic fluorescent protein for repression in *Cac* resulted in up to 90% reduction in fluorescence in comparison to their control [64], but it is difficult to draw a direct comparison, as this is data on the functional protein level, not on the transcript level as we have. Our results therefore suggest that d*Fn*Cas12a can achieve gene repression at levels at least comparable to d*Spy*Cas9.

In previous studies, the metabolic profile reported upon disruption of the *dha* operon has varied. Pyne *et al*. were the first to report the simultaneous production of 1,2-PDO and 1,3-PDO in *Cpa,* and reported an increase in 1,2-PDO when the *dhaT2* was disrupted using a TargeTron system. The resulting strain also showed reduced ethanol production and increased butanol and acid production compared to their wild-type control [65]. In a separate study, allele coupled exchange was applied to *Cpa* for the complete deletion of the *dhaBCE* genes. The resulting strain showed complete abolition of 1,3-PDO but recorded no significant increase of butanol [62]. Interestingly, while the ACE deletion strain could not be grown in Biebl medium, whose composition is known to drive flux toward 1,3-PDO production, Pyne *et al.* attributed the unaffected growth of their strain in a semi-defined medium to the redox balance afforded by increased production of 1,2-PDO.

In this study, we observed no long-term growth inhibition in cultures where d*Fn*Cas12a was targeted to the *dha* operon. However, we were not able to inhibit 1,3-PDO production in the long-term nor observe transcriptional repression when targeting *dhaB* upon d*Fn*Cas12a induction (Fig. S5). Silvis *et al.* [53] demonstrated that *mreB*, an essential gene in *E. coli,* is able to evade transcriptional control of CRISPR-based gene repression systems via a negative transcriptional feedback loop. In their study, expression of *mreB* initially decreased with basal expression of an appropriate single-guide RNA but recovered to wild type levels with time. 1,3-Propanediol production is tightly regulated in several bacterial species including *Clostridium pasteurianum* [66] and based on our results alone, it is difficult to ascertain whether the transient reduction in 1, 3-PDO production we observe is a result of d*Fn*Cas12a activity or a separate event of unknown cause. However, a feedback loop could potentially explain why long-term repression of *dha* operon is not observed in this study in spite of the 1,3-PDO reduction observed shortly after d*Fn*Cas12a induction. Silvis *et al.* were able to overcome the endogenous *mreB* feedback loop by increasing expression of the single-guide RNA. For the experiments in this study, we induced d*Fn*Cas12a with 10 mM lactose based on previous studies [13,67]. Broader use of our d*Fn*Cas12a system for transcriptional repression may require the employment of inducible promoters with a wider dynamic range in order to overcome endogenous transcriptional feedback mechanisms.

4.2. dFnCa12a system as a tool to determine gene function

The results of our study remain consistent with previous publications

as it relates to the repression of *adc*. Down regulation or deletion of *adc* has generally resulted in a significant decrease, though not complete eradication of acetone production and a decrease in the re-assimilation of acids to alcohols. In addition, we observed reduced growth and glucose consumption, previously attributed to pH crash (Fig. S4). The simultaneous downregulation of *adc* and *pdc* however, reduced acetone and butanol production to undetectable concentrations. These observations suggest that under the growth conditions used here, and in the absence of Adc, *pdc* expression facilitates solvent production. While no knock-out studies have been reported for *pdc* in *Clostridium acetobutylicum*, our d*Fn*Cas12a system allowed us to, each in a single round of cloning and transformations, elucidate metabolic profiles for reduced *pdc* expression, in addition to, that of simultaneously reduced *pdc* and *adc* expression.

In *Clostridium acetobutylicum*, acetone is produced in a two-step process. In the first step, acetoacetyl-CoA is converted to acetoacetate via acetoacetyl-CoA transferase (CtfAB). The production of acetoacetate is coupled to acid re-assimilation as CtfAB utilizes either acetate or butyrate as the CoA acceptor during this reaction [68]. In a previous study Dharani *et al.* showed that the expression of heterologous *pdc* in *Clostridium acetobutylicum* not only increased acetone production, but also increased acid re-assimilation. This study further supports the phenotypic role of Pdc in solvent production and allowed rapid phenotypic characterization of simultaneous *adc* and *pdc* down-regulation in *Clostridium acetobutylicum*.

Traditional knockout methods in *Clostridium* species are facilitated by low efficiency double crossover events and often require multiple rounds of cloning for knockouts with multiple targets being deleted consecutively [11]. Additionally, the use of Cas12a as a selective marker for isolating double crossover events, even when multiple genes are targeted simultaneously, requires large repair templates for each region targeted [28]. The use of a synthetic CRISPR array to concurrently target multiple genes for repression allows quick and facile characterization of genotype-to phenotype relationships that can lead to an overall better understanding of *Clostridium* species and identification of targets for rational genome editing that would lead to desired strains.

5. Conclusion

We demonstrate here successful utilization of d*Fn*Cas12a CRISPR interference for gene repression in two *Clostridium* species. In *Clostridium acetobutylicum* we achieved over 99% reduction in mRNA levels, nearing abolished expression of targeted genes. We show of our CRISPRi system for multiplexed gene repression through the simultaneous reduction of *adc* and *pdc*, revealing a unique metabolic profile, compared to when these genes are individually repressed.

While we were able to demonstrate downregulation of genes in *Clostridium pasteurianum*, targeting *hydA* did not present with the metabolic profile that has been established in previous. Other CRISPR-based gene repression studies in *Clostridium* have also shown inconsistencies in the level of transcriptional repression compared to the phenotypical difference observed [30,52]. This indicates that regulation on a translational level remains a valuable way to study gene and protein function in the absence of a more fundamental understanding of endogenous gene regulation mechanisms, specifically for tightly regulated genes and operons.

This CRISPRi tool based on d*Fn*Cas12a is a useful addition to the mesophilic *Clostridium* genetic toolkit. It has shown to be capable of strong gene repression, but will benefit from an improved heuristic for guide RNA designs in the future, as these are a major factor in repression level.

Conflict of interest statement

The authors declare no conflict of interest.

CRediT authorship contribution statement

Rochelle Carla Joseph: Methodology, Investigation, Data curation, Visualization, Writing – original draft. **Nicholas R. Sandoval:** Conceptualization, Supervision, Writing – review & editing, Funding acquisition.

Declaration of competing interest

The authors declare no conflicts of interest.

Acknowledgements

This work was supported by NSF CBET Award 1847226. The authors wish to thank Nick Benner and Caroline Duncan for assistance in laboratory work.

Appendix A. Supplementary data

Supplementary data to this article can be found online at https://doi.org/10.1016/j.synbio.2022.12.005.

References

[1] Jones SW, et al. CO2 fixation by anaerobic non-photosynthetic mixotrophy for improved carbon conversion. Nat Commun 2016;7:12800.
[2] Poehlein A, et al. Microbial solvent formation revisited by comparative genome analysis. Biotechnol Biofuels 2017;10(1):58.
[3] Baral NR, Shah A. Techno-economic analysis of cellulosic butanol production from corn stover through acetone–butanol–ethanol fermentation. Energy Fuels 2016;30(7):5779–90.
[4] Wen Z, et al. Improved n-butanol production from Clostridium cellulovorans by integrated metabolic and evolutionary engineering. Appl Environ Microbiol 2019;85(7).
[5] Qi F, et al. Improvement of butanol production in Clostridium acetobutylicum through enhancement of NAD(P)H availability. J Ind Microbiol Biotechnol 2018;45(11):993–1002.
[6] Wen Z, et al. Metabolic engineering of Clostridium cellulovorans to improve butanol production by consolidated bioprocessing. ACS Synth Biol 2020;9(2):304–15.
[7] Rotta C, et al. Closed genome sequence of Clostridium pasteurianum ATCC 6013. Genome Announc 2015;3(1).
[8] Enany S. Structural and functional analysis of hypothetical and conserved proteins of Clostridium tetani. J Infect Public Health 2014;7(4):296–307.
[9] Lacey JA, et al. Whole genome analysis reveals the diversity and evolutionary relationships between necrotic enteritis-causing strains of Clostridium perfringens. BMC Genom 2018;19(1):379.
[10] Patakova P, et al. Acidogenesis, solventogenesis, metabolic stress response and life cycle changes in Clostridium beijerinckii NRRL B-598 at the transcriptomic level. Sci Rep 2019;9(1):1371.
[11] Joseph RC, Kim NM, Sandoval NR. Recent developments of the synthetic biology toolkit for Clostridium. Front Microbiol 2018;9. 154-154.
[12] Kim NM, Sinnott RW, Sandoval NR. Transcription factor-based biosensors and inducible systems in non-model bacteria: current progress and future directions. Curr Opin Biotechnol 2020;64:39–46.
[13] Al-Hinai MA, Fast AG, Papoutsakis ET. Novel system for efficient isolation of Clostridium double-crossover allelic exchange mutants enabling markerless chromosomal gene deletions and DNA integration. Appl Environ Microbiol 2012;78(22):8112–21.
[14] Ehsaan M, et al. Mutant generation by allelic exchange and genome resequencing of the biobutanol organism Clostridium acetobutylicum ATCC 824. Biotechnol Biofuels 2016;9(1):4.
[15] Heap JT, et al. The ClosTron: a universal gene knock-out system for the genus Clostridium. J Microbiol Methods 2007;70(3):452–64.
[16] Xu T, et al. Cas9 nickase-assisted RNA repression enables stable and efficient manipulation of essential metabolic genes in Clostridium cellulolyticum. Front Microbiol 2017;8:1744.
[17] Nakayama S, et al. Metabolic engineering for solvent productivity by downregulation of the hydrogenase gene cluster hupCBA in Clostridium saccharoperbutylacetonicum strain N1-4. Appl Microbiol Biotechnol 2008;78(3):483–93.
[18] Pyne EM, et al. Antisense-RNA-mediated gene downregulation in Clostridium pasteurianum. Fermentation 2015;1(1).
[19] Jinek M, et al. A programmable dual-RNA-guided DNA endonuclease in adaptive bacterial immunity. Science 2012;337(6096):816–21.
[20] Zetsche B, et al. Cpf1 is a single RNA-guided endonuclease of a class 2 CRISPR-Cas system. Cell 2015;163(3):759–71.
[21] Zetsche B, et al. Multiplex gene editing by CRISPR–Cpf1 using a single crRNA array. Nat Biotechnol 2016;35:31.

[22] Zhang J, et al. Optimizing a CRISPR-Cpf1-based genome engineering system for Corynebacterium glutamicum. Microb Cell Factories 2019;18(1):60.
[23] Marshall R, et al. Rapid and scalable characterization of CRISPR Technologies using an E. coli cell-free transcription-translation system. Mol Cell 2018;69(1):146–57. e3.
[24] Tu M, et al. A 'new lease of life': FnCpf1 possesses DNA cleavage activity for genome editing in human cells. Nucleic Acids Res 2017;45(19):11295–304.
[25] Zhong Z, et al. Plant genome editing using FnCpf1 and LbCpf1 nucleases at redefined and altered PAM sites. Mol Plant 2018;11(7):999–1002.
[26] Swiat MA, et al. FnCpf1: a novel and efficient genome editing tool for Saccharomyces cerevisiae. Nucleic Acids Res 2017;45(21):12585–98.
[27] To´th E, et al. Mb- and FnCpf1 nucleases are active in mammalian cells: activities and PAM preferences of four wild-type Cpf1 nucleases and of their altered PAM specificity variants. Nucleic Acids Res 2018;46(19):10272–85.
[28] Joseph RC, et al. Metabolic engineering and the synthetic biology toolbox for Clostridium. Metabolic Engineering; 2021. p. 611–51.
[29] Qi Lei S, et al. Repurposing CRISPR as an RNA-guided platform for sequence-specific control of gene expression. Cell 2013;152(5):1173–83.
[30] Zhao R, et al. CRISPR-Cas12a-Mediated gene deletion and regulation in Clostridium ljungdahlii and its application in carbon flux redirection in synthesis gas fermentation. ACS Synth Biol 2019;8(10):2270–9.
[31] Gao L, et al. Engineered Cpf1 variants with altered PAM specificities. Nat Biotechnol 2017;35(8):789–92.
[32] Ran FA, et al. In vivo genome editing using Staphylococcus aureus Cas9. Nature 2015;520(7546):186–91.
[33] Zhang Y, et al. Processing-independent CRISPR RNAs limit natural transformation in Neisseria meningitidis. Mol Cell 2013;50(4):488–503.
[34] Garneau JE, et al. The CRISPR/Cas bacterial immune system cleaves bacteriophage and plasmid DNA. Nature 2010;468(7320):67–71.
[35] Esvelt KM, et al. Orthogonal Cas9 proteins for RNA-guided gene regulation and editing. Nat Methods 2013;10(11):1116–21.
[36] Heap JT, et al. A modular system for Clostridium shuttle plasmids. J Microbiol Methods 2009;78(1):79–85.
[37] Cobb RE, Wang Y, Zhao H. High-efficiency multiplex genome editing of Streptomyces species using an engineered CRISPR/Cas system. ACS Synth Biol 2015;4(6):723–8.
[38] Mermelstein LD, et al. Expression of cloned homologous fermentative genes in Clostridium acetobutylicum ATCC 824. Biotechnology (N Y) 1992;10(2):190–5.
[39] Mermelstein LD, Papoutsakis ET. In vivo methylation in Escherichia coli by the Bacillus subtilis phage phi 3T I methyltransferase to protect plasmids from restriction upon transformation of Clostridium acetobutylicum ATCC 824. Appl Environ Microbiol 1993;59(4):1077–81.
[40] Pyne ME, et al. Development of an electro transformation protocol for genetic manipulation of Clostridium pasteurianum. Biotechnol Biofuels 2013;6(1):50.
[41] Sandoval NR, et al. Whole-genome sequence of an evolved Clostridium pasteurianum strain reveals Spo0A deficiency responsible for increased butanol production and superior growth. Biotechnol Biofuels 2015;8(1):227.
[42] Bustin SA, et al. The MIQE guidelines: minimum information for publication of quantitative real-time PCR experiments. Clin Chem 2009;55(4):611–22.
[43] Jones SW, et al. The transcriptional program underlying the physiology of clostridial sporulation. Genome Biol 2008;9(7):R114.
[44] Specht DA, Xu Y, Lambert G. Massively parallel CRISPRi assays reveal concealed thermodynamic determinants of dCas12a binding. Proc Natl Acad Sci U S A 2020;117(21):11274–82.
[45] Zhang W, et al. The off-target effect of CRISPR-Cas12a system toward insertions and deletions between target DNA and crRNA sequences. Anal Chem 2022;94(24):8596–604.
[46] Kim H, et al. Enhancement of target specificity of CRISPR-Cas12a by using a chimeric DNA-RNA guide. Nucleic Acids Res 2020;48(15):8601–16.
[47] Cui L, et al. A CRISPRi screen in E. coli reveals sequence-specific toxicity of dCas9. Nat Commun 2018;9(1):1912.
[48] Zhou Y, et al. CRISPR-Cas12a-Assisted genome editing in amycolatopsis mediterranei. Front Bioeng Biotechnol 2020;8:698.
[49] Zhang J, et al. Efficient multiplex genome editing in streptomyces via engineered CRISPR-Cas12a systems. Front Bioeng Biotechnol 2020;8:726.
[50] Harris LM, Welker NE, Papoutsakis ET. Northern, morphological, and fermentation analysis of spo0A inactivation and overexpression in Clostridium acetobutylicum ATCC 824. J Bacteriol 2002;184(13):3586–97.
[51] Al-Hinai MA, Jones SW, Papoutsakis ET. σK of Clostridium acetobutylicum is the first known sporulation-specific sigma factor with two developmentally separated roles, one early and one late in sporulation. J Bacteriol 2014;196(2):287–99.
[52] Fackler N, et al. Transcriptional control of Clostridium autoethanogenum using CRISPRi. Synth Biol 2021;6(1):ysab008.
[53] Silvis MR, et al. Morphological and transcriptional responses to CRISPRi knockdown of essential genes in Escherichia coli. mBio 2021;12(5). e0256121-e0256121.
[54] Jiang Y, et al. Disruption of the acetoacetate decarboxylase gene in solvent-producing Clostridium acetobutylicum increases the butanol ratio. Metab Eng 2009;11(4):284–91.
[55] Buddrus L, et al. Crystal structure of pyruvate decarboxylase from Zymobacter palmae. Acta Crystallogr. Sect. F Struct. Biol. Commun. 2016;72(Pt 9):700–6.
[56] Hossain MA, et al. Characterization of pyruvate decarboxylase genes from rice. Plant Mol Biol 1996;31(4):761–70.
[57] Mücke U, et al. Pyruvate decarboxylase from Pisum sativum. Eur J Biochem 1996;237(2):373–82.
[58] Ishchuk OP, et al. Overexpression of pyruvate decarboxylase in the yeast Hansenula polymorpha results in increased ethanol yield in high-temperature fermentation of xylose. FEMS Yeast Res 2008;8(7):1164–74.
[59] Grimmler C, et al. Genome-wide gene expression analysis of the switch between acidogenesis and solventogenesis in continuous cultures of Clostridium acetobutylicum. J Mol Microbiol Biotechnol 2011;20(1):1–15.
[60] Dharani SR, et al. Engineering Clostridium acetobutylicum for enhanced solvent production by overexpression of pyruvate decarboxylase from Zymomonas mobilis. Appl Biochem Microbiol 2021;57(5):611–7.
[61] Ventura J-RS, Hu H, Jahng D. Enhanced butanol production in Clostridium acetobutylicum ATCC 824 by double overexpression of 6-phosphofructokinase and pyruvate kinase genes. Appl Microbiol Biotechnol 2013;97(16):7505–16.
[62] Schwarz KM, et al. Towards improved butanol production through targeted genetic modification of Clostridium pasteurianum. Metab Eng 2017;40:124–37.
[63] Li Q, et al. CRISPR-based genome editing and expression control systems in Clostridium acetobutylicum and Clostridium beijerinckii. Biotechnol J 2016;11(7):961–72.
[64] Bruder MR, et al. Extending CRISPR-Cas9 technology from genome editing to transcriptional engineering in genus Clostridium. Appl Environ Microbiol 2016;82(20):6109–17.
[65] Pyne ME, et al. Disruption of the Reductive 1,3-Propanediol Pathway Triggers Production of 1,2-Propanediol for Sustained Glycerol Fermentation by Clostridium pasteurianum. Appl Environ Microbiol 2016;82(17):5375–88.
[66] Johnson EE, Rehmann L. The role of 1,3-propanediol production in fermentation of glycerol by Clostridium pasteurianum. Bioresour Technol 2016;209:1–7.
[67] Hartman AH, Liu H, Melville SB. Construction and characterization of a lactose-inducible promoter system for controlled gene expression in Clostridium perfringens. Appl Environ Microbiol 2011;77(2):471–8.
[68] Andersch W, Bahl H, Gottschalk G. Level of enzymes involved in acetate, butyrate, acetone and butanol formation by Clostridium acetobutylicum. Eur J Appl Microbiol Biotechnol 1983;18(6):327–32.